EXTRACELLULAR BIOSYNTHESIS OF SILVER NANOPARTICLES BY *TRICHODERMA REESEI* AND THEIR APPLICATION TO REMOVE XANTHOGENATE FROM WASTEWATER

O. Ts. Gemishev[1]*, M. I. Panayotova[2], V. T. Panayotov[2], E. S. Zaharieva[1]

[1]Department of Biotechnology, Faculty of Biology, Sofia University "St. Kliment Ohridski", Sofia, Bulgaria

[2]Department of Chemistry, University of Mining and Geology, Sofia, Bulgaria

Abstract

Application of fungi in the biosynthesis of silver nanoparticles is a green and feasible alternative to chemical and physical methods used for AgNPs synthesis. The fungus Trichoderma reesei is a non-pathogenic and environmentally friendly microorganism capable to produce extracellular enzymes and metabolites in high scale. An extracellular biosynthesis of silver nanoparticles (AgNPs) from $AgNO_3$ solution by using the cell-free extract of Trichoderma reesei biomass is presented in this study. Kinetics of the biotransformation is described by a second order reaction equation. Spherical or approximately spherical AgNPs that are well-dispersed and with a size between 3-4 and 15-17 nm have been produced at transformation degree of 30 % with respect to the initial silver ions concentration. The biosynthesized AgNPs show high stability against agglomeration even after storage for 60 days. Soluble xanthates, used in some industrial applications, are found toxic to aquatic biota even at low concentrations. The synthesized AgNPs are capable to immobilize potassium amyl xanthate from model wastewater. The pollutant adsorption is described by the Langmuir adsorption isotherm and the calculated maximum adsorption capacity is 4.67 mg/mg. The pollutant immobilization by AgNPs is much faster process and requires much less adsorbent (50 fold) in comparison with the activated carbon (chemical grade of purity).

Keywords: *silver nanoparticles, biosynthesis, Trichoderma reesei, potassium amyl xanthate removal*

1. INTRODUCTION

Nanosized particles have attracted the interest of scientific community due to their unique properties. Silver is one of metals often used for production of nanoparticles for different environmental applications, such as water disinfection, removal of pollutants from water, gas sensing etc. All those applications require stable, non-aggregable and in many cases non-hydrophobic nanoparticles. The Ag nanoparticles (AgNPs) can be synthesized by diverse physical (evaporation-condensation, laser ablation) and chemical (by use of organic and inorganic reducing agents) routes. In recent years the green synthesis of AgNPs is emphasized. It includes the use of plant extracts, and extracts from microbial sources like bacteria, fungi, algae and yeast. The biosynthesis method is considered to be "green", i.e. clean, nontoxic and environmentally acceptable.

The green synthesis of nanoparticles by fungi is thought as an important method due to the presence of a variety of enzymes in their cells and the simple handling. High rate of specific metabolite production, fast growth rate, easy, safe and efficient harvesting arrange the fungi among the most suitable candidates for metal nanoparticles synthesis.

Seventy percent of fungi which have been studied as AgNPs biosynthesis agents are pathogenic for plant, human or animals [1]. Their use requires measures and costs to deal with their side negative effects on human society and the environment.

Some *Trichoderma* species are a good example of nonpathogenic fungi for safe and environmentally friendly production of AgNPs. Extracellular biosynthesis of AgNPs has been realized by using *T. asperellum* [2], *T. viride* [3], *T. atroviride* [4], *T. harizianum* [5], *T. koningii* [6]. The fungus *Trichoderma reesei* is a non-pathogenic, environmentally friendly microorganism with high scale

production of extracellular enzymes [7]. *Trichoderma reesei* for its own survival produces extracellular reductase enzymes which reduce toxic silver ions (Ag^+) to nontoxic AgNPs [1] The fungus is recognized for its high growth rate, capability for large-scale production and low-cost requirement for production procedures.

Studies on *Trichoderma*-based synthesis of AgNPs are still limited [4]. That is why in the present study, an extracellular biosynthesis of AgNPs from $AgNO_3$ solution by using cell-free extract (CFE) of *T. reesei* biomass has been performed.

Certain xanthate salts are used as flotation reagents in mineral processing. Xanthates are used to control radical polymerization [8]. Some antiviral medicines can be prepared based on xanthates [9]. The mentioned and other industrial applications can lead to a release of water polluted with xanthates. Under ambient environmental conditions, the half-life of xanthate is approximately four days. Xanthates are toxic to aquatic biota at concentrations of 1.5 mg/L [10]. Waste streams bearing residual xanthates should not be discharged to natural water-bodies without additional treatment.

Different methods have been proposed for xanthate removal from wastewater. Fenton reagent was used in the degradation experiments of remainder xanthate (125 mg/L) in flotation wastewater. The xanthate removal was 99.5 % under the conditions of oxidation time of 60 min, initial pH 4, and concentrations of reagents: Fe^{2+} - 20 mg/L and H_2O_2 - 20 mg/L [11]. Beneficiation wastewater containing butyl xanthate was treated by oxidation with sodium hypochlorite. The removal rate of 99.05 % was reached at initial pH 4, reaction time of 50 min, and sodium hypochlorite 120 mg/L [12]. The removal of butyl xanthate by catalytic ozonation process using Mn-Ce-Al_2O_3 catalyst was studied. The removal ratio of 98.72 % was achieved at initial pH =7.22, 1.75 g/h of ozone dosage, 0.5 g/L of catalyst loading, 100 mg/L of initial butyl xanthate concentration, and reaction time of 8 min [13]. Sorption is considered an environmentally friendly and relatively cheap method for water treatment. Modified bentonite adsorbents were synthesized and used for the removal of the residual potassium amyl xanthate from the synthetic solutions at adsorbent dosage 7500 mg/L, xanthate concentration 2000 mg/L, pH=12.2, 45 min [14]. Under optimum conditions Al-modified bentonite removed 99% of the residual xanthate.

However, xanthate removal, when it presents in relatively low concentrations and at neutral pH of the fluid subjected to the treatment, still needs further attempts. In the present study we have decided to test the capability of the synthesized AgNPs to immobilize potassium amyl xanthate from model wastewater and to compare it with the xanthate adsorption on the activated carbon.

2. MATERIALS AND METHODS

2.1. Fungus cultivation and biosynthesis of AgNPs

Experiment was conducted with culture of *Trichoderma reesei* cultivated on potato-dextrose agar (PDA) at 28±1°C for seven days.

The fungal biomass was obtained after inoculating the strain in 100 mL of growth media containing: glucose – 2 %, NH_4Cl 0.1 %, $CO(NH_2)_2$ - 0.3 %, $(NH_4)_2SO_4$ – 0.1 %, KH_2PO_4 - 0.2 %, $(NH_4)_2SO_4$ - 0.14 %, $MgSO_4$. $7H_2O$ - 0.03 %, $CaCl_2$. $2H_2O$ - 0.04 % , and 0.1 % corn steep liquor. The fungal culture was incubated in 500 cm^3 flasks at 29±1 °C for 72 h, under continuous shaking at 220 rpm. After that the fungus biomass was separated from the culture broth by sterile Whatman No. 1 filter paper and washed multiple times with sterile distilled water. Then 10% of the wet biomass was suspended in 200 mL sterile distilled H_2O and it was extracted for 24 h, under continuous shaking at 150 rpm. After that the utilized fungus biomass was again separated. Silver nitrate (p.a.) – $AgNO_3$ was dissolved in the obtained CFE, containing a mixture of fungus metabolites, to yield overall Ag^+ ions concentration of 10 mM.

The extracellular cell-free biosynthesis of AgNPs was carried out in 500 cm^3 flasks, in dark condition, at 29±1°C, under continuous shaking at 150 rpm. The process was followed for 168 hours by taking

samples at every 24 h. Additional measurements were made after 60 days (1440 h) of storage at room temperature of samples containing CFE, $AgNO_3$ and AgNPs.

2.2. AgNPs characterization

The process of AgNPs formation was monitored by UV-Vis absorption spectroscopy. BOECO S-220 UV/VIS spectrophotometer was used at the wavelength from 200 to 700 nm (1 nm interval). Three milliliters of the CFE, containing the synthesized AgNPs, were taken at every 24 hours and their absorbance was recorded. Further, the obtained AgNPs were isolated by centrifugation (30 min, 13300 rpm), washed several times with distilled water, re-suspended and their spectra were also recorded.

The amount of bio-transformed Ag^+ was measured by Inductively-Coupled Plasma-Atomic Emission Spectroscopy (ICP-AES) after dissolving the AgNPs isolated from known volume of CFE, containing the synthesized AgNPs.

The synthesized and isolated nanoparticles were characterized by X-ray Photoelectron Spectroscopy (XPS), Transmission Electron Microscopy (TEM) and Fourier transform infrared spectroscopy (FTIR). The surface charge of synthesized AgNPs was found by using zeta potential measurements.

The XPS measurements were carried out with electron spectrometer Escalab-MkII (VG Scientific) with a base pressure of 1 x 10^{-10} mbar. The spectra were excited with AlK_α radiation ($h\nu$ = 1486.6 eV) at instrumental resolution of 1.1 eV as measured by FWHM of $Ag3d_{5/2}$ photoelectron line. Energy calibration was made by using the strongest O1s line in the spectra centered at 532.7 eV. To carry out the measurement the isolated and washed AgNPs were placed on a Si plate. For the TEM analysis washed AgNPs were re-suspended in distilled water**.** A drop of thus obtained mixture was casted on carbon-coated copper grids and allowed to dry under vacuum prior the measurement. The characterization was carried out on JEOL model JEM 2100, 200 kV analytical electron microscope. For the FTIR analysis, biosynthesized AgNPs were triply washed with distilled water, followed by triply washing in ethyl alcohol and drying overnight under dark conditions at 40 ^oC. After that 2 mg of sample was mixed with 200 mg potassium bromide (FTIR grade), pressed into a pellet and placed into the sample holder. The FTIR spectra were scanned in the range 4000 – 400 cm^{-1} at a resolution of 1 cm^{-1} by using Perkin Elmer spectrophotometer. For the zeta-potential measurements isolated, washed and air-dried AgNPs were re-suspended in distilled water, then sonicated for 10–20 min to disperse the particles. Malvern Nano-ZS 90 analyzer was used.

2.3. Adsorption experiments

Solutions containing different concentrations of potassium amyl xanthate ($CH_3(CH_2)_4OCS_2K$) were prepared by dissolving $CH_3(CH_2)_4OCS_2K$ (p.a.) in distilled water. Experiments were conducted batch-wise - corresponding amounts of AgNPs suspension were added to 50 mL of xanthate solution in order to obtain concentrations of AgNPs equal to 2.5 and 5 mg/L. In comparative studies with activated carbon (Sigma Aldrich, 20-40 mesh) the adsorbent was added to xanthate solution to obtain concentrations 50 and 250 mg/L. The solutions were stirred with magnetic stirrer. Aliquot portions were taken at particular time (10, 15, 30, 60, 120, 180 min) and the amount of xanthate remained in the solution was determined by UV spectrometry. Absorption at 301 nm where aqueous solutions of xanthate have an absorbance maximum and corresponding preliminary prepared calibration line was used.

2.4. Equations used

The degree of Ag^+ biotransformation was calculated by the following expression:

$$Ag^+ \text{ biotransformed, } \% = (C_i / C_o) \times 100, \qquad (1)$$

where C_o – initial concentration of Ag^+ and C_i – the Ag concentration determined by ICP.

Experimental data have been fitted to the equations describing first and second order irreversible reactions [15].

For the first order irreversible reactions:

$$\ln C_t = - k \times t + \ln C_o \qquad (2)$$

where C_o and C_t - initial and at time t reactant concentration, k - rate constant [$time^{-1}$] .

For the second order irreversible reactions:

$$1 / C_t = k \times t + 1 / C_o \qquad (3)$$

where k is the reaction rate constant [concentration x $time^{-1}$]; C_o, C_t and t - as described above.

In adsorption experiments the pollutant removal from the initial solution, was calculated using the equation (4):

$$\text{Removal, \%} = [(C_o-C_t) /C_o] \times 100 \qquad (4)$$

where C_o is the initial and C_t is the pollutant concentration at time t, mg/L.

The quantity of immobilized pollutant q_t (mg/g) is calculated according to equation (5):

$$q_t = [(C_o-C_t) \times V / m] \qquad (5)$$

where C_o is the initial concentration and C_t is the residual concentration of the pollutant at time t (mg/L), m is the mass of the adsorbent (mg) and V is the volume of the solution, contacting with the adsorbent. When equilibrium is reached the relation gives the amount q_e, (mg/mg) of pollutant immobilized per unit mass of the adsorbent at equilibrium:

$$q_e = [(C_o-C_e) \times V / m] \qquad (5')$$

and C_e is the residual concentration of the pollutant at equilibrium (mg/L).

Freundlich and Langmuir isotherm equations were tested for their ability to describe the adsorption equilibrium. The isotherms were used in their linear form:

Freundlich equation:

$$\log q_e = \log K_F + 1/n \times \log C_e \qquad (6)$$

where q_e, and C_e - as described above, K_F - Freundlich constant [$mg^{(1-1/n)} \times L^{1/n} / g$] or given as [(mg/g) / $(L/mg)^{1/n}$],

Langmuir equation:

$$C_e / q_e = 1 / (K_L \times q_{max}) + C_e / q_{max} \qquad (7)$$

where q_{max} (mg/mg) is the maximum adsorption capacity, and K_L is the Langmuir equilibrium constant (L/mg) related to the energy of adsorption, q_e, and C_e - as described above.

3. RESULTS AND DISCUSSION

3.1. AgNPs growth

UV–Vis spectra of the solutions containing CFE, $AgNO_3$ and AgNPs recorded at different time are presented in Fig. 1a. Spectra of the isolated, washed and re-suspended AgNPs are given in Figure 1b.

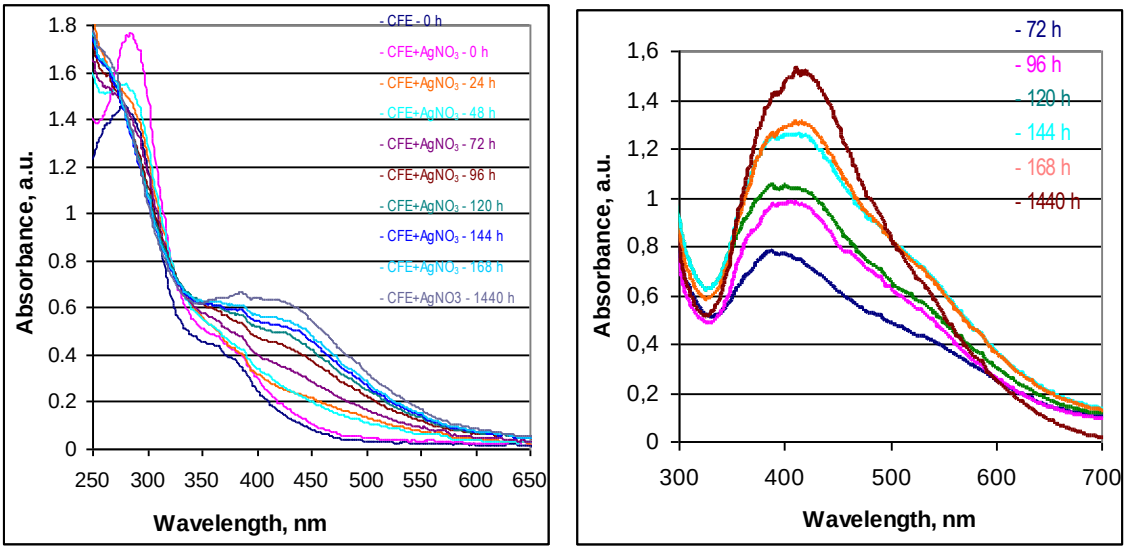


Fig. 1. UV–Vis spectra of (at left) solutions containing CFE, $AgNO_3$ and AgNPs, (at right) isolated, washed and re-suspended AgNPs

A well pronounced peak around 280 nm can be seen (Fig 1a) in the beginning of the experiments. It can be related to the superposition of the absorption bands of proteins and $AgNO_3$. The intensity of this peak decreases in time implying transformation of the components of the reaction medium. Simultaneously a broad peak appears, starting at 370-380 nm and indicating the presence of AgNPs. Its intensity increases with the time which indicates the continued reduction of the silver ions and an increase in concentration of AgNPs. This can be seen well in Fig. 1b. The position of observed peaks can be related with relatively small AgNPs, as reported also by other authors [4, 16] and confirmed by the TEM analysis – Fig. 3.

The observed increase in intensity of the absorbance peak with time indicates the continued reduction of the silver ions and an increase in concentration of AgNPs. The intensity of the plasmon peak initially increases faster with number of days of incubation due to increasing concentration of the silver nanoparticles (since the intensity of the plasmon peak is proportional to the concentration of produced AgNPs). Further in time the peak increase was small and this could be assigned to nearly completion of the reaction. A slight redshift in the peak position is observed. It is most pronounced between 72nd and 96th hour of incubation but continues till 144 h suggesting of some growth of nanoparticles [17]. This was confirmed also by TEM (see Fig. 3). Further, the redshift in the peak is practically negligible, even after 1440 h. This implies stabilization of the AgNPs size, most probably due to the particles capping by suitable capping species (identified by FTR). This was confirmed by the stability of the solution containing CFE, $AgNO_3$ and AgNPs, kept at room temperature for 60 days and showing no evidence of aggregation of particles.

Kinetics of Ag^+ biotransformation is presented in Fig. 2. The initially pale yellow CFE containing $AgNO_3$ started changing colour from the second day of incubation onwards and turned brown by the end of the sixth day. The kinetic curve is described by the equation for the second order reaction (R^2 = 0.922), pointing that the process depends on the availability of two different species - $AgNO_3$ and the reducing and capping reagent(s) from the CFE. Other authors also reported a second order reaction of Ag^+ reduction by cell-free filtrate of *Trichoderma asperellum* [2].

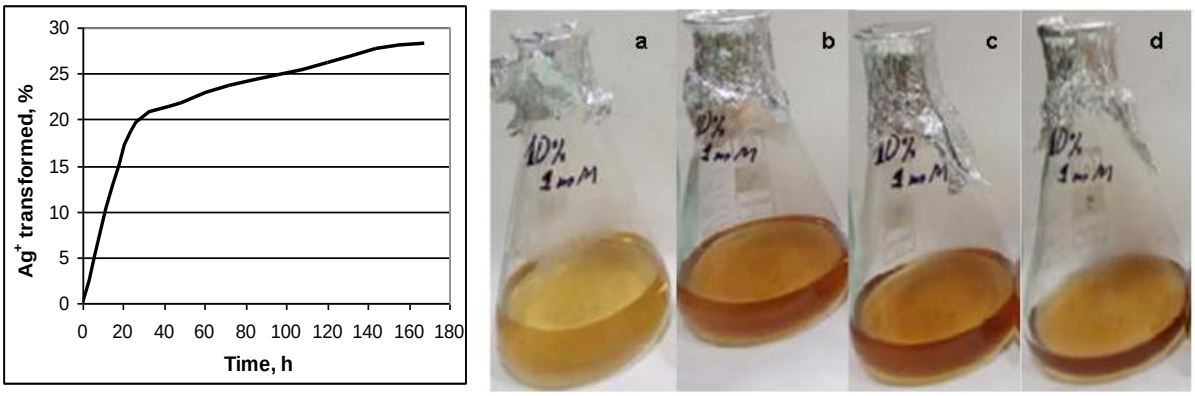


Fig. 2. Kinetics of Ag^+ biotransformation: at left - kinetic curve; at right - change in the solution color: a - after 24 h, b after 72 h, c after 96 h, d - after 144 h

Most probably in the beginning, the concentration of $AgNO_3$ was relatively high and its consumption during the course of its reduction was practically negligible, leading to a linear dependence of concentration of the product with time. As the reaction proceeded, the concentration of $AgNO_3$ decreased and its concentration term in the rate equation was no longer negligible compared to the other reactants - the fact that is manifested in the nonlinearity of the curve.

3.2. AgNPs characterization

The XPS spectra (Ag3d photoelectron) of isolated bio-synthesized AgNPs showed a peak at binding energy (BE) of 368.3 eV. Since the binding energy of the Ag3d5/2 and Ag3d3/2 doublet for metallic silver is observed at 368.3 eV and 374.3 eV, respectively [18] the peaks detected is our case indicate formation of Ag^o.

The zeta potential of the prepared AgNPs was found to be -47.4 mV. The value is of the same range as found for AgNPs synthesized by *Trichoderma harzianum* [5]. A zeta potential value of over ±30 mV is considered optimal for avoiding agglomerates formation [19]. The high negative value of the zeta potential ensures repulsion among the AgNPs and thereby increases their stability. Actually, even after storage for 60 days, no obvious discoloration of the solution or visible agglomeration of the AgNPs was observed which points at the AgNPs stability. The latter may be due to the proteins on the surface of the AgNPs. By using FTIR analysis the following functional groups of the protein molecules, wrapping AgNPs and acting as capping reagents, were identified: hydroxy, amine, methyl, carboxylate, ether [20]. TEM images of prepared AgNPs are presented in Fig. 3.

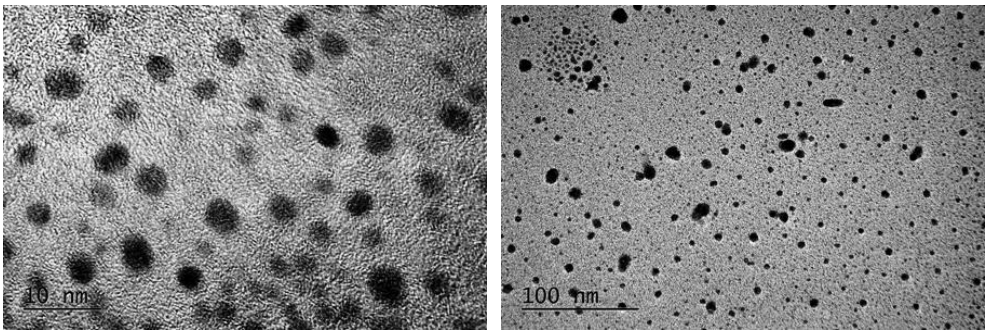


Fig. 3. TEM images of prepared AgNPs: at left - after 72 h of reduction, at right - after 144 h of reduction

As it can be seen in Fig. 3, TEM measurements demonstrated that AgNPs were spherical or approximately spherical, well-dispersed and with a size between 3-4 (at 72 h) and 15-17 (at 144 h) nm.

These findings correspond to the observed small redshift in the wave length of the recorded UV peaks (see Fig. 1). Similar effects were observed also by other authors [2, 17]. However, even bigger particles are with relatively low size. This implies that the enzymes extracted from the biomass act not only as reducing but also as a capping reagent.

3.3. AgNPs use

Data on the impact of the AgNPs amount and time on the potassium amyl xanthate removal from the water are presented in Fig. 4.

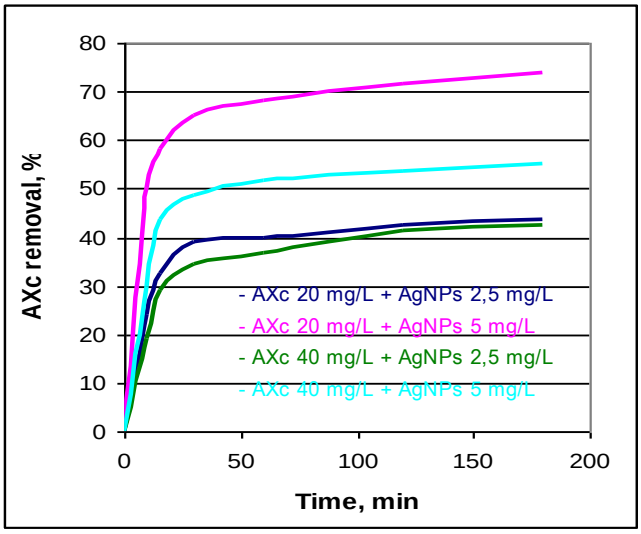


Fig. 4. Potassium amyl xanthate removal from water - impact of the used amount of biosynthesized AgNPs

As it can be seen in Fig. 4, an increase in the dose of the used AgNPs leads to an increase in the amount of the immobilized pollutant. This fact is obvious at two different initial concentrations of the pollutant. That is why the further experiments with other initial pollutant concentrations were carried out with the higher AgNPs dose, i.e. 5 mg/L. The influence of the initial pollutant concentration on the removal is presented in Fig. 5.

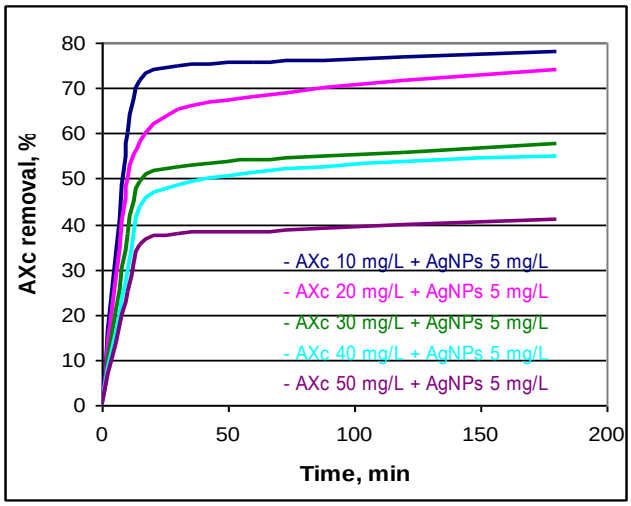


Fig. 5. Potassium amyl xanthate removal from water by use of biosynthesized AgNPs - impact of the initial pollutant concentration

An increase in the initial pollutant's concentration leads to a decrease in the AXc removal, expressed as a per cent of the initial concentration. However, the amount of immobilized xanthate increase with increasing the initial pollutant's concentration, practically until reaching the adsorption capacity of the AgNPs which is near to the maximum one calculated by using the Langmuir isotherm (see below).

Experimental data fitting to the isotherm equations showed that the process is best described by the Langmuir isotherm with R^2 = 0.983 - Fig. 6. The data best-fitting to the Langmuir model indicates a monolayer adsorption of xanthate on the AgNPs [14]. The maximum calculated adsorption capacity of the biosynthesized AgNPs, calculated using the isotherm equation is quite high, i.e. q_{max}= 4.67 mg/mg. This could be related with the small diameter of the AgNps ensuring high adsorption surface at relatively low mass of the adsorbent.

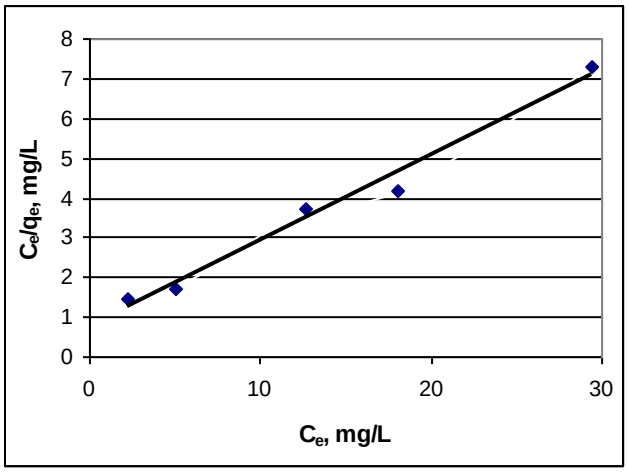


Fig. 6. Langmuir isotherm for adsorption of potassium amyl xanthate on biosynthesized AgNPs

Comparative experiments have been carried out on potassium amyl xanthate removal by adsorption on "classical" adsorbent for organic pollutants, namely - with high quality activated carbon. Data obtained on the removal of potassium amyl xanthate by adsorption on activated carbon are presented in Fig. 7.

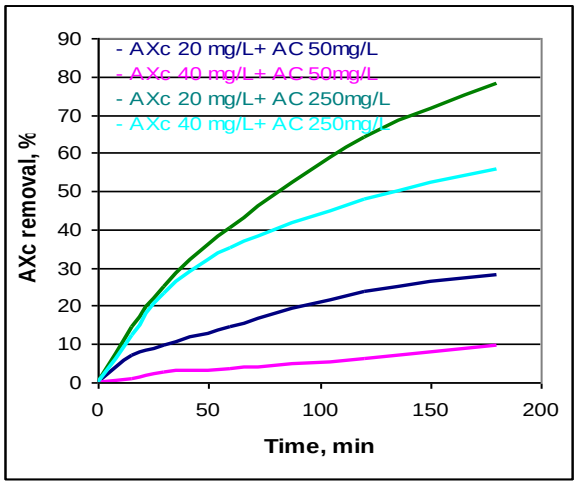


Fig. 7. Potassium amyl xanthate removal from water by use of activated carbon

By collating the data presented in Figures 5 and 7, it can be stated that the pollutant immobilization by the activated carbon is much slower process and requires much more adsorbent in comparison with the biosynthesized AgNPs. For example, at initial potassium amyl xanthate concentration of 20 mg/L a removal of 60 % is achieved in approximately 20 min with AgNPs, practically not achieved with 50 mg/L activated carbon (10 fold higher concentration compared to that of the AgNPs) and achieved in 110 min with 250 mg/L activated carbon (50 fold higher concentration compared to that of the AgNPs). At initial potassium amyl xanthate concentration of 40 mg/L a removal of over 50 % is achieved in approximately 60 min with AgNPs, not achieved with 50 mg/L activated carbon, and 180 min were needed to obtain this removal with 250 mg/L activated carbon.

CONCLUSIONS

1. We have successfully biosynthesized spherical or approximately spherical AgNPs that are well-dispersed and with a size between 3-4 (at 72 h) and 15-17 (at 144 h) nm with the aid of CFE of the fungus *Trichoderma reesei*. Kinetics of the biotransformation is described by a second order reaction equation.
2. The CFE contains functional groups which act as green capping reagents, thus ensuring the small size of the produced AgNPs and contributing to their stability against agglomeration.
3. The biosynthesized AgNPs possess relatively high zeta potential that ensures their stability against agglomeration even after storage for 60 days.
4. The proposed AgNPs synthesis method is economically viable and environmentally sustainable. However, further work is needed to improve the efficiency of synthesis, the control of particle size and morphology and to speed the process before its implementation in the real life.
5. The biosynthesized AgNPs exhibited better ability, compared to good quality activated carbon, to immobilize an organic pollutant, namely potassium amyl xanthate, from water solutions. The pollutant adsorption is best described by the Langmuir adsorption isotherm and the maximum adsorption capacity is calculated as 4.67 mg/mg. The pollutant immobilization by AgNPs is much faster process and requires much less adsorbent (50 fold) in comparison with the activated carbon.

ACKNOWLEDGEMENTS

The authors thank the National Science Fund of Bulgaria for the financial support of the project DN-17/20.

REFERENCES

1. Vahabi, K & Dorcheh SK 2014, Biosynthesis of Silver Nano-Particles by *Trichoderma* and Its Medical Applications, in Gupta, VK, Schmoll, M, Herrera-Estrella, A, Upadhyay, RS, Druzhinina, I, Tuohy, MG (eds), Biotechnology and Biology of *Trichoderma,* Elsevier B.V., pp. 393-404.
2. Mukherjee, P, Roy, M, Mandal, BP, Dey, GK, Mukherjee, PK, Ghatak, J., Tyagi AK & Kale, SP 2008, 'Green synthesis of highly stabilized nanocrystalline silver particles by a non-pathogenic and agriculturally important fungus *T. Asperellum', Nanotechnology,* vol. 19, 075103, 7 pp.
3. Elgorban, AM, Al-Rahmah, AN, Sayed, SR, Hirad, A, Mostafa AAF & Bahkali, AH 2016, 'Antimicrobial activity and green synthesis of silver nanoparticles using *Trichoderma viride', Biotechnology & biotechnology equipment*, vol. 30, no. 2, pp. 299-304.
4. Saravanakumar, K, Wang, MH 2018, 'Trichoderma based synthesis of anti-pathogenic silver nanoparticles and their characterization, antioxidant and cytotoxicity properties', *Microbial Pathogenesis,* vol. 114, pp. 269–273.
5. Ahluwalia, V, Kumar, J, Sisodia, R, Shakil, NA & Walia, S 2014, 'Green synthesis of silver nanoparticles by *Trichoderma harzianum* and their bio-efficacy evaluation against Staphylococcus aureus and Klebsiella pneumonia', *Industrial Crops and Products*, vol. 55, pp. 202–206.
6. Tripathi, RM Gupta, RK, Shrivastav, A, Singh, MP, Shrivastav BR & Singh P 2013, '*Trichoderma koningii* assisted biogenic synthesis of silver nanoparticles and evaluation of their antibacterial activity', *Advances in Natural Sciences: Nanoscience and Nanotechnology*, vol. 4**,** 035005, 5 pp.
7. Oksanen T, Pere J, Paavilainen L, Buchert J, Viikari L 2000, 'Treatment of Recycled Kraft Pulps with *Trichoderma Reesei* Hemicellulases and Cellulases', *J Biotechnol,* vol. 78, no. 1, pp. 39–48.
8. Laot, Y 2011, 'Nouvelles applications de la chimie radicalaire des xanthates a la synthese' heterocycles azotes'. PhD thesis, Ecole Polytechnique X, Paris.
9. Sauer, G, Amtmann, E, Melber, K, Knapp, A, Műller, K, Hummel, K & Scherm A 1984, 'DNA and RNA Virus Species are Inhibited by Xanthates, a Class of Antiviral Compounds with Unique Properties', *Proc. Natl. Acad. Sci USA*, vol. 81, no. 11, pp. 3263-3267.
10. Xu, Y, Lay, JP & Korte F 1988, 'Fate and effects of xanthates in laboratory freshwater systems', *Bull. Environ. Contam. Toxicol*, vol. 41, no. 5, pp. 683-689.
11. Xu, J, Sun, S, Zhang, P & Cai H 2005, 'Degradation of remainder xanthate in flotation wastewater by Fenton reagent', *Environmental Protection of Chemical Industry*, vol. 2, pp. 63-69.
12. Qun, Y, Jun-wen, H, Mei-xiang, T & Yang, Y., 2011, 'Experimental study on the treatment of butyl xanthate from beneficiation wastewater by sodium hypochlorite', *Proceedings Electric Technology and Civil Engineering (ICETCE) International Conference*, pp. 1262 – 1264.
13. Zhang, Y, Wu, C, Lin, Z & Lin, J, 2011, 'Catalytic ozonation of mineral processing wastewater containing butyl xanthate', *Proceedings Computer Distributed Control and Intelligent Environmental Monitoring (CDCIEM) Int. Conference* pp. 1998 – 2001.
14. Massinaei, RRM & Moghaddam, AZ 2018, 'Removal of the residual xanthate from flotation plant tailings using modified bentonite', *Minerals Eng.*, vol. 119, pp. 1-10.
15. Atkins, PW & De Paula, J 2006, *Physical Chemistry for the Life Sciences*, Freeman and Company, New York.
16. Fayaz, M, Tiwary, CS, Kalaichelvan PT & R. Venkatesan, 2010, 'Blue orange light emission from biogenic synthesized silver nanoparticles using *Trichoderma viride', Colloids and Surfaces B: Biointerfaces*, vol. 75, pp. 175–178.
17. Gade, A, Gaikwad, S, Duranc, N & Rai, M 2014, 'Green synthesis of silver nanoparticles by Phoma glomerata', *Micron*, vol. 59, 52–59.

18. Perkin-Elmer Corporation 1992, *Handbook of X-ray photoelectron spectroscopy*, Physical electronics, Minnesota.
19. Fernández, J, Fernández-Baldoc, MA, Berni, E, Camí, G, Duránd, N, Raba, J & San MI 2016, 'Production of silver nanoparticles using yeasts and evaluation of theirantifungal activity against phytopathogenic fungi', *Process Biochemistry*, vol. 51, pp.1306–1313.
20. Coates, J 2006, Interpretation of Infrared Spectra, A Practical Approach, in R.A. Meyers (ed.), *Encyclopedia of Analytical Chemistry; Applications, Theory and Instrumentation*, John Wiley & Sons Ltd, pp.1-23.